Electronic Supplementary Information

A Chemical Circular Communication Network at the Nanoscale

*Beatriz de Luis, Ángela Morellá-Aucejo, Antoni Llopis-Lorente, Tania M. Godoy-Reyes, Reynaldo Villalonga, Elena Aznar, Félix Sancenón, and Ramón Martínez-Máñez**

1. Chemicals

Tetraethyl orthosilicate (TEOS), *n*-cetyltrimethylammonium bromide (CTABr), sodium hydroxide (NaOH), gold(III) chloride trihydrate ($HAuCl_4 \cdot 3H_2O$), sodium citrate tribasic dihydrate, (3-mercaptopropyl)trimethoxysilane, paraffin wax, 3-mercaptopropionic acid, tris(2,2'-bipyridyl)dichlororuthenium(II) hexahydrate ($[Ru(bpy)_3]Cl_2 \cdot 6H_2O$), 2,2'-dipyridyl disulfide, O-(2-mercaptoethyl)-O'-methyl-hexa(ethylene glycol), β-galactosidase from *Aspergillus oryzae*, methyl 4-(bromomethyl)benzoate, 3-(triethoxysilyl)propyl isocyanate, 4-(hydroxymethyl) phenyl boronic acid pinacol ester, galactose oxidase from *Dactylium dendroides*, sodium, tris(2-carboxyethyl)phosphine hydrochloride, (3-iodopropyl)trimethoxysilane, benzimidazole, triethylamine, β-cyclodextrin, esterase from porcine liver, *N*-(3-dimethylaminopropyl)-*N'*-ethylcarbodiimide hydrochloride (EDC), *N*-hydroxysuccinimide (NHS), D-(+)-galactose, D-(+)-lactose monohydrate, glucose oxidase from *Aspergillus niger*, 2,2'-azino-bis(3-ethylbenzothiazoline-6-sulfonic acid) diammonium salt (ABTS), peroxidase from horseradish (HRP) and 4-nitrophenyl butyrate were purchased from Sigma-Aldrich and used without further purification.

Sodium sulfate anhydrous, sodium dihydrogen phosphate monohydrate, disodium hydrogen phosphate heptahydrate, ethanol, chloroform, toluene, acetonitrile and anhydrous tetrahydrofuran were provided by Scharlau.

2. General methods

Powder X-ray diffraction (PXRD), transmission electron microscopy (TEM), N_2 adsorption-desorption isotherms, UV-visible and fluorescence spectrophotometry, dynamic light scattering (DLS) and elemental analysis techniques were employed for materials characterization. PXRD measurements

were performed on a Seifert 3000TT diffractometer using CuKα radiation at low angles ($1.3 < 2\theta < 8.3$, with steps of 0.04 degrees and 3 seconds for step) and high angles ($35 < 2\theta < 80$ with steps of 0.04 degrees and 1 second for step). TEM images were acquired using a JEOL TEM-1010 Electron microscope working at 100 kV. Additionally, TEM coupled with energy dispersive X-ray spectroscopy (TEM-EDX) was used for element mapping using a JEOL TEM-2100F microscope. ^{1}H spectra were recorded at 400 MHz on a Bruker 400 Avance III Spectrometer. DLS studies were performed using a ZetaSizer Nano ZS (Malvern). N_2 adsorption-desorption isotherms were recorded on a Micromeritics TriStar II Plus automated analyzer. Samples were previously degassed at 90 °C in vacuum overnight and measurements were performed at 77 °K. UV-visible spectra were recorded with a JASCO V-650 spectrophotometer. Fluorescence measurements were carried out in a JASCO FP-8500 spectrophotometer. Elemental analysis was performed using a LECO CHNS-932 Elemental Analyzer.

3. Synthesis of the self-immolative arylboronate (1)

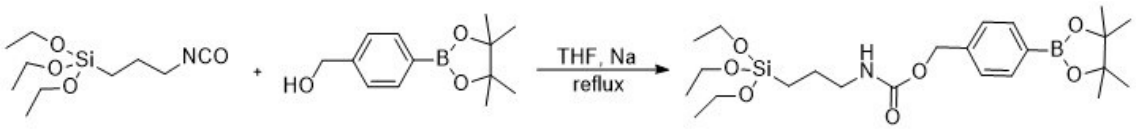

Figure S1. Synthesis of self-immolative arylboronate derivative (**1**).

4-(Hydroxymethyl) phenyl boronic acid pinacol ester (235 mg, 1.01 mmol) was dissolved in anhydrous THF (8 mL) and a small piece of Na (ca. 1 mg) was added. After stirring 10 min under argon at room temperature, (3-isocyanatopropyl)triethoxysilane (249 µL, 1.01 mmol) was added dropwise and the mixture was stirred under reflux for 24 h. Then, the solvent was evaporated and sodium salts were removed with a CH_2Cl_2/H_2O extraction. This procedure led to the self-immolative molecule (**1**) with an 75% yield as a dark yellow oil.

^{1}H NMR (300 MHz, $CDCl_3$) δ 7.78 (d, 2H), 7.33 (d, 2H), 5.10 (s, 2H), 3.79 (m, 6H), 3.18 (m, 2H), 1.62 (m, 2H), 1.34 (s, 12H), 1.21 (m, 9H), 0.62 (m, 2H), in accordance to previous literature.[1]

4. Synthesis of mesoporous silica nanoparticles (MSNPs)

1.00 g (2.74 mmol) of *n*-cetyltrimethylammonium bromide (CTABr) was dissolved in 480 mL of deionized water. Then, the pH was basified by adding 3.5 mL of a 2 mol·L^{-1} NaOH solution and the temperature was increased to 80 °C. Next, tetraethyl orthosilicate (TEOS) (5 mL, 22.4 mmol) was added dropwise into the solution. Magnetic stirring was kept for 2 hours to give a white suspension. Finally, the solid was isolated by centrifugation, washed several times with water until neutral pH and dried at 70 °C overnight (as-synthesized MSNPs). To obtain the final mesoporous nanoparticles (**MSNPs**), the

as-synthesized solid was calcined at 550 °C in an oxidant atmosphere for 5 hours in order to remove the surfactant.

5. Synthesis of gold nanoparticles

Gold nanoparticles were synthesized following the Turkevich-Frens method.[2,3] 100 mL of a 0.3 mM $HAuCl_4 \cdot 3H_2O$ solution were brought to 135 °C under stirring and refluxing. Then, 1.5 mL of a 1 % sodium citrate solution was added to yield gold nanoparticles of ca. 20 nm. The initially pale-yellow colour turned to purple-black and finally red wine in 10 minutes. After this, the colloidal suspension was cooled to room temperature under stirring. This protocol was repeated 4 times until obtaining 400 mL of the colloidal gold nanoparticles suspension.

6. Synthesis of Janus Au-MS nanoparticles (S0)

180 mg of MCM-41 type mesoporous silica nanoparticles (**MSNPs**) were dispersed in 9 mL of an aqueous solution (6.7 % ethanol) followed by addition of *n*-cetyltrimethylammonium bromide (CTABr, 1 μM). The mixture was heated at 75 °C, and then 1 g of paraffin wax was added. Once the paraffin was melted, the mixture was vigorously stirred for 15 minutes using a homogenizer (Ultra-Turrax T-8, IKA). Then, the mixture was further stirred for 1 hour at 75 °C using a magnetic stirrer. The resulting Pickering emulsion was then cooled to room temperature, diluted with 10 mL of methanol and reacted with 200 μL of (3-mercaptopropyl)trimethoxysilane for 3 hours. The solid was collected by centrifugation and washed with methanol. For gold attachment, the partially mercapto-functionalized nanoparticles were dispersed in 68 mL of methanol and added over the 400 mL of the colloidal gold nanoparticles suspension previously synthesized. The mixture was stirred overnight at room temperature. Then, the solid was isolated by filtration and exhaustively washed with chloroform and hexane. The solid was dried and ground. This process finally yielded the Janus Au-mesoporous silica nanoparticles (Janus Au-MS nanoparticles, **S0**).

7. Synthesis of S1

For the preparation of **S1**, 50 mg of **S0** and 25 mg of $[Ru(bpy)_3]Cl_2 \cdot 6H_2O$ dye were suspended in acetonitrile (3 mL, 13 mM) and stirred overnight in order to achieve the loading of the pores. Then, the solid was isolated by centrifugation, washed with acetonitrile and dried under vacuum. Afterwards, in order to protect the gold face, this loaded solid was resuspended in ethanol (5 mL) and let to react with 70 μL of 3-mercaptopropionic acid stirring for 1 hour at room temperature. The solid was isolated by centrifugation, washed twice with ethanol and allowed to air dry. Next, the resulting solid was resuspended in anhydrous acetonitrile (1.7 mL) and (3-mercaptopropyl)trimethoxysilane (93 μL, 0.5

mmol) was added. The suspension was stirred for 5.5 hours at room temperature and then, 2,2'-dipyridyl disulfide (110 mg, 0.5 mmol) was added to the reaction mixture. After stirring overnight at room temperature, the resulting solid was centrifuged, washed twice with acetonitrile and dried under vacuum. Finally, a mixture of this prepared solid and O-(2-mercaptoethyl)-O'-methyl-hexa(ethylene glycol) (50 µL, 0.15 mmol) was suspended in acetonitrile (3.33 mL) and was stirred overnight. The final capped Janus nanoparticles **S1** were isolated by centrifugation, washed with abundant acetonitrile and dried under vacuum.

8. Synthesis of $S1_{\beta gal}$

8 mg of **S1** were suspended in 2 mL of 50 mM sodium phosphate buffer at pH 7.5. Then, 2.5 mg of *N*-(3-dimethylaminopropyl)-*N'*-ethylcarbodiimide hydrochloride (EDC), 2.5 mg of *N*-hydroxysuccinimide (NHS) and 10 mg of the enzyme β-galactosidase were added and the suspension was stirred overnight at 10 °C. The solid was isolated by centrifugation and washed several times with cold 50 mM sodium phosphate buffer (pH 7.5). The resulting $\mathbf{S1_{\beta gal}}$ was kept wet in refrigerator until use.

9. Synthesis of S2

In order to prepare the solid **S2**, 25 mg of **S0** were suspended in 1.8 mL of acetonitrile and treated with 25 µL of 3-mercaptopropionic acid to functionalize the gold face. The solution was stirred for 1 hour and then nanoparticles were isolated and washed twice by centrifugation with fresh acetonitrile. Once dried under vacuum, these nanoparticles (25 mg) were loaded by stirring for 24 h under argon atmosphere in 5 mL of anhydrous acetonitrile containing 24 mg of methyl 4-(bromomethyl)benzoate (21 mM). Then, the self-immolative molecule (**1**) (70 mg, 0.14 mmol) was dissolved in 700 µL of anhydrous acetonitrile and added dropwise to the nanoparticle suspension. The mixture was let to react for 5.5 h stirring at room temperature. Afterwards, the solid was isolated by centrifugation, washed twice with acetonitrile, twice with PBS buffer 5X (pH 7.5) and dried under vacuum overnight. The resulting nanoparticles and 90 mg of β-cyclodextrin were mixed in 5 mL of PBS buffer 5X (pH 7.5) and stirred overnight. Finally, the nanoparticles were isolated by centrifugation, washed 3 times with PBS buffer 5X (pH 7.5) and dried under vacuum. This process finally yielded the solid **S2**.

10. Synthesis of $S2_{galox}$

5 mg of **S2** were suspended in 1.4 mL of 50 mM sodium phosphate buffer at pH 7.5. Then, 1 mg of EDC, 1 mg of NHS and 100 µL of the commercial enzyme solution galactose oxidase were added and the suspension was stirred overnight at 10 °C. The solid was isolated by centrifugation and washed several

times with cold 50 mM sodium phosphate buffer (pH 7.5). The resulting **S2$_{galox}$** was kept wet in refrigerator until use.

11. Synthesis of S2$_{blank}$

Solid **S2$_{blank}$** was prepared following the same procedure described for **S2$_{galox}$** but the mesoporous container was not loaded.

12. Synthesis of S3

For the preparation of **S3**, 60 mg of **S0** were suspended in anhydrous acetonitrile (4 mL) and reacted with 60 µL of (3-iodopropyl) trimethoxysilane for 5.5 hours. The solid was isolated by centrifugation, washed with acetonitrile and dried at 70 °C overnight. To functionalize the surface with benzimidazole moieties, 0.25 g of benzimidazole and 990 µL of triethylamine were mixed with 20 mL of toluene and heated for 20 min at 80 °C in order to prepare a saturated solution of benzimidazole. 10 mL of this suspension were added over 60 mg of the previously prepared nanoparticles. The mixture was stirred at 80 °C for three days. Afterward, the benzimidazole-functionalized solid was isolated by centrifugation and washed with toluene. To protect the gold face, the resulting solid was suspended in 5 mL of acetonitrile and reacted with 50 µL of 3-mercaptopropionic acid for 1 hour. This solid was centrifuged, washed with toluene and with water and let to dry at 70 °C overnight. Next, the loading process was carried out by suspending the solid in 8 mL of a concentrated solution in 50 mM phosphate buffer at pH 7.5 of tris(2-carboxyethyl)phosphine hydrochloride (25 mg, 12.5 mM). The solid was centrifuged, washed twice with 50 mM phosphate buffer at pH 7.5, once with ethanol and dried under vacuum. Finally, the solid was suspended with 20 mg of β-cyclodextrin in 12.5 mL of 50 mM sodium phosphate buffer at pH 7.5 and stirred overnight. The suspension was centrifuged, washed thoroughly with 50 mM phosphate buffer at pH 7.5 and dried under vacuum. This process finally yielded the solid **S3**.

13. Synthesis of S3$_{est}$

8 mg of **S3** were suspended in 4 mL of 50 mM sodium phosphate buffer at pH 7.5. Then, 2.5 mg of EDC, 2.5 mg of NHS and 2 mg of the enzyme esterase were added and the suspension was stirred overnight at 10 °C. The solid was isolated by centrifugation and washed several times with cold 50 mM sodium phosphate buffer (pH 7.5). The resulting **S3$_{est}$** was kept wet in refrigerator until use.

14. Synthesis of S3$_{blank}$

Solid **S3$_{blank}$** was prepared following the same procedure described for **S3$_{est}$** but the mesoporous container was not loaded.

15. Characterization

Solids were characterized by standard techniques.

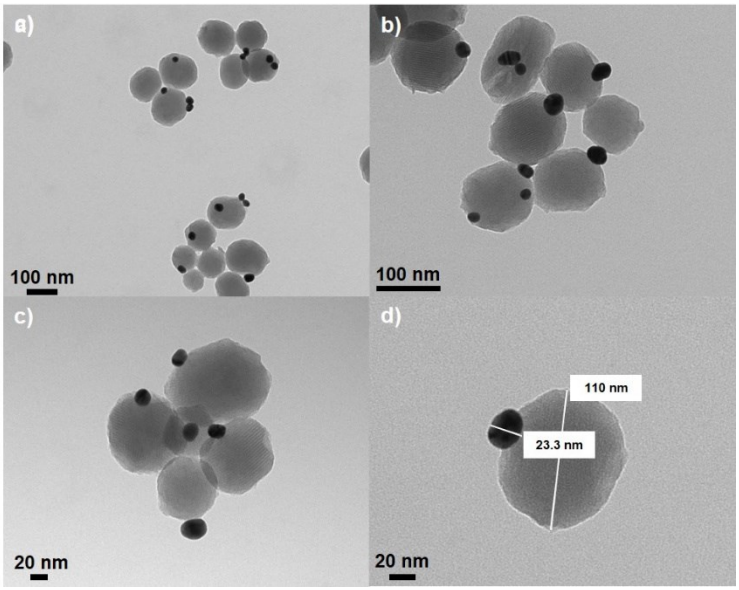

Figure S2. Additional TEM images of the Janus Au-MS nanoparticles **S0** (a-d).

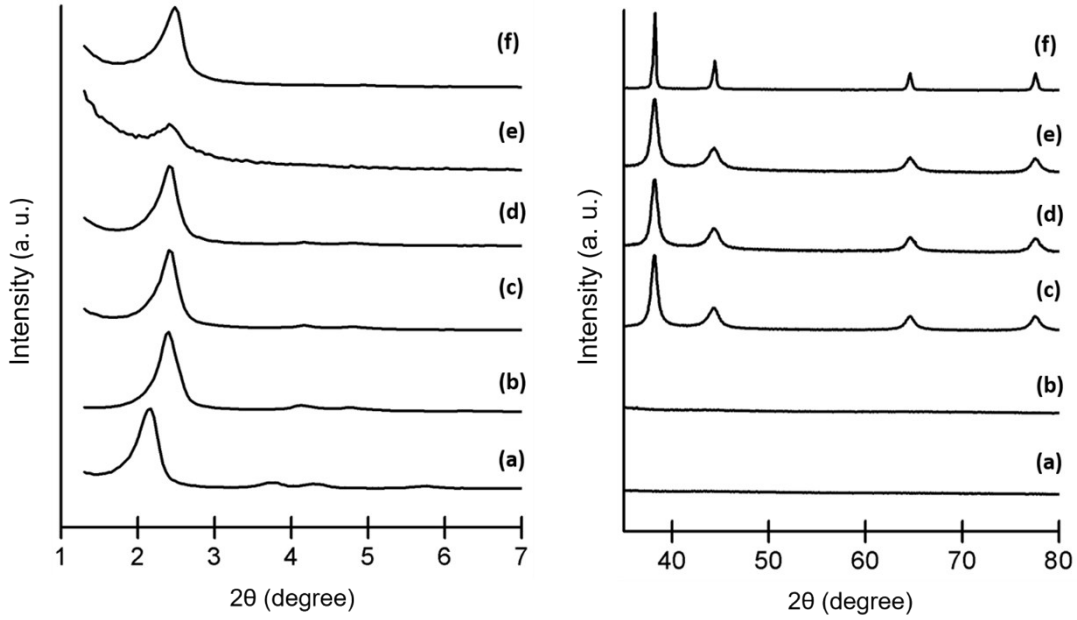

Figure S3. Powder X-ray diffraction patterns of the solids (a) **as-made MSNPs**, (b) **calcined MSNPs**, (c) Janus Au-MS nanoparticles **S0**, (d) solid **S1**, (e) solid **S2** and (f) solid **S3** at low (left) and high (right) angles.

Figure S3 shows powder X-ray diffraction patterns at low ($1.5 < 2\theta < 7$) and at high angles ($35 < 2\theta < 80$) of different prepared nanoparticles. At low angles, the as-made **MSNPs** shows characteristic low-

angle reflections of mesoporous silica. In **calcined MSNPs** a slight displacement of the peaks related to the condensation of silanol groups during the calcination process was observed. These low-angle typical peaks are preserved in the Janus Au-MS nanoparticles **S0**. The presence of the (100) peak in the PXRD patterns in the solid **S1**, **S2** and **S3** indicated that the different chemical modifications, functionalization and cargo loading had not damaged the mesoporous structure. Moreover, the high-angle diffraction pattern of the Janus colloids **S0**, **S1**, **S2** and **S3** showed the cubic gold characteristic (111), (200), (220) and (331) diffraction peaks, confirming the presence of gold nanocrystals in the Janus Au-mesoporous silica architecture.[4] Powder X-ray diffraction pattern of nanoparticles containing enzymes were not obtained due to the low quantity collected in the synthesis but the mild enzyme immobilization procedure is not expected to affect the Janus Au-mesoporous silica architecture.

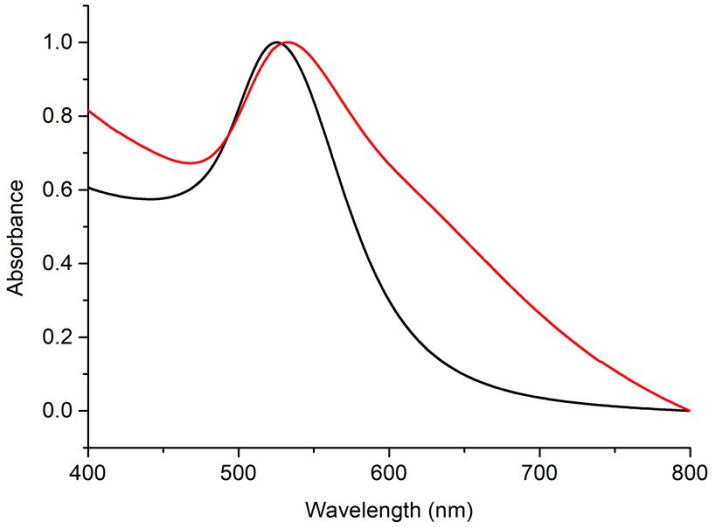

Figure S4. Normalized UV-Visible spectra of the gold nanoparticles (black) and Janus Au-MS nanoparticles **S0** (red).

UV/vis measurements in aqueous solution were performed on the as-synthesized gold nanoparticles and on Janus Au-MS nanoparticles **S0** (by suspending 1 mg of solid in 1 mL of distilled water). The starting gold colloid showed a single absorption band at 524 nm, characteristic of the surface plasmon resonance of spherically shaped nanospheres with approximately 20 nm diameter. In the **S0** spectrum, there is a redshift of the absorbance maximum (533 nm) and a broadening of the band when compared with the as-synthesized gold nanoparticles. These two facts can be ascribed to the increase in the refractive index around the gold nanospheres due to the mesoporous silica attachment and to light refraction produced by silica.[5]

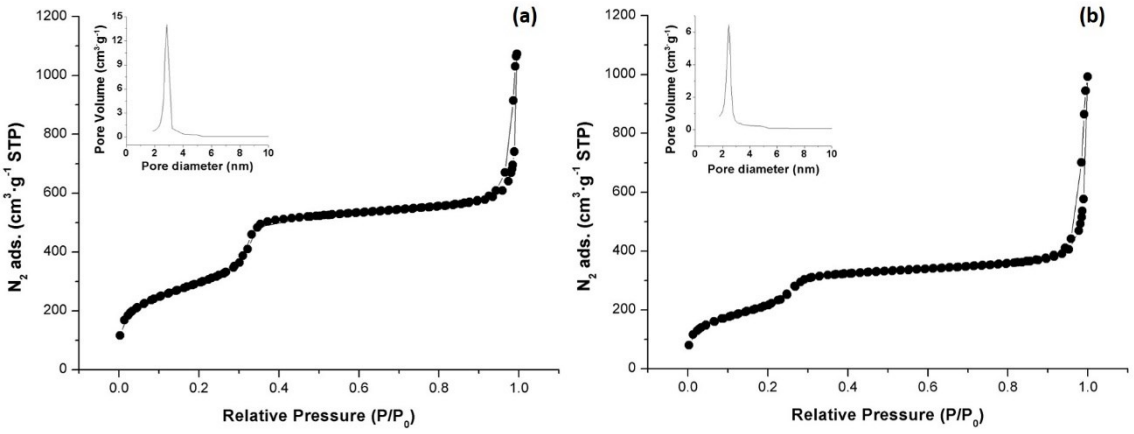

Figure S5. The N_2 adsorption-desorption isotherms for (a) the **calcined MSNPs** and (b) Janus Au-MS nanoparticles **S0**.

The N_2 adsorption-desorption isotherms of the **calcined MSNPs** and Janus Au-MS nanoparticles **S0** show an adsorption step at intermediate P/P_0 value 0.3, which is characteristic for mesoporous solids with empty pores. This step is related to the nitrogen condensation inside the mesopores by capillarity. The absence of a hysteresis loop in this interval and the narrow BJH pore distribution suggest the existence of uniform cylindrical mesopores. Application of the BET model resulted in a value for the total specific surface of 1079 $m^2 \cdot g^{-1}$ for **calcined MSNPs** and 802 $m^2 \cdot g^{-1}$ for Janus Au-MS nanoparticles **S0**. In order to calculate pore size and total pore volume, BJH model was applied on the adsorption band of the isotherm for $P/P_0 < 0.6$ (associated to adsorption inside the pores). BET specific values, pore volumes and pore sizes calculated from N_2 adsorption-desorption isotherms for **MSNPs** and Janus Au-MS nanoparticles **S0** are listed in **Table S1**.

Table S1. BET specific surface values, pore volumes and pore sizes calculated from N_2 adsorption-desorption isotherms for selected materials.

Solid	S_{BET} [$m^2 \cdot g^{-1}$]	Pore Volume [$cm^3 \cdot g^{-1}$]	Pore size [nm]
Calcined MSNPs	1079 ± 1	0.92	2.72
S0	802 ± 6	0.60	2.43

The zeta potential and hydrodynamic size of different solids were measured by dynamic light scattering (DLS) studies (**Table S2** and **Figure 2C** in main text, respectively). For carrying out the experiments, the

corresponding materials were suspended in distilled water at pH 7 at a concentration of 0.01 $mg \cdot mL^{-1}$.

Table S2. Zeta potential values determined by DLS for the different materials.

Sample	Zeta Potential (mV)
MSNPs	-29.7 ± 1
S0	-28.4 ± 0.5
S1	-35.2 ± 0.8
S2	-18.2 ± 1.2
S3	-36.7 ± 0.9
$\mathbf{S1}_{\beta gal}$	-31.3 ± 0.9
$\mathbf{S2}_{galox}$	-26.3 ± 0.4
$\mathbf{S3}_{est}$	-30.4 ± 0.7

From elemental analysis data (**Table S3**), composition of solids was calculated. Considering the data obtained from the analysis of **S1**, the amount of oligo(ethylene glycol) grafted onto the mesoporous silica face was determined as 69.6 $mg \cdot g^{-1}$ of solid. The amount of $[Ru(bpy)_3]Cl_2$ loaded was estimated to be 70.9 $mg \cdot g^{-1}$ from delivery studies. From the analysis of **S2**, the amount of self-immolative molecular gate was determined to be 261.4 $mg \cdot g^{-1}$ of solid. The cargo was estimated by measuring the absorbance of methyl 4-(bromomethyl)benzoate remaining in solution (λ_{abs} = 243 nm in ACN; λ_{abs} = 244 nm in PBS buffer pH 7.5) during the steps for the synthesis of **S2**. The calibration curves indicate and amount of 83.3 mg of methyl 4-(bromomethyl)benzoate per g of **S2**. From the analysis of **S3**, the amount of $(CH_2)_3$-benzimidazole was determined as 12.5 $mg \cdot g^{-1}$ of solid and the cargo tris(2-carboxyethyl)phosphine was estimated to be 9.7 $mg \cdot g^{-1}$.

Table S3. Elemental analysis data.

Solid	% C	% H	% N	% S
S0	1.84	2.02	0.13	0.38
S1	6.68	2.22	0.93	1.25
S2	8.69	2.46	1.15	0.31
S3	2.28	1.57	0.22	0.27

The immobilization of the enzymes was confirmed by running the corresponding enzyme activity assay and was calculated by applying the following formula:

$$\frac{Enzyme\ Units}{g} = \frac{(\Delta\ -\ \Delta_{blank}) \cdot V_T \cdot F_D}{\varepsilon_{chromop.} \cdot l \cdot V_S \cdot C_S}$$

Where, Δ is the slope of the graph (min^{-1}); Δ_{blank} is the slope of the graph for the blank (min^{-1}); V_T is the total volume in the cuvette; F_D is the dilution factor; $\varepsilon_{chromop.}$ is the molar extinction of the corresponding chromophore at a defined wavelength ($M^{-1} \cdot cm^{-1}$); L is the optical path in the cuvette (1 cm); V_S is the volume of the sample added (mL); C_S is the concentration of sample added ($g \cdot mL^{-1}$).

The method we used in order to test β-galactosidase activity is based on the cleavage of lactose by β-galactosidase into galactose and glucose. Then, the glucose is oxidized by glucose oxidase leading to gluconic acid and hydrogen peroxide. Hydrogen peroxide reacts with ABTS (2,2'-azino-bis(3-ethylbenzothiazoline-6-sulfonic acid) diammonium salt) in the presence of peroxidase (HRP) to form a blue-green product ($ABTS^{\cdot+}$) that can be followed UV-visible spectrophotometry (λ_{abs} = 418 nm).

Reactions for assaying β-galactosidase activity:

$$D\text{-}lactose + H_2O \xrightarrow{\beta\text{-Galactosidase}} D\text{-}glucose + D\text{-}galactose$$
$$D\text{-}glucose + O_2 + H_2O \xrightarrow{\text{Glucose oxidase}} D\text{-}gluconic\ acid + H_2O_2$$
$$H_2O_2 + ABTS \xrightarrow{\text{HRP}} ABTS^{\cdot+} + H_2O$$

In a typical experiment to check β-galactosidase activity, 250 µL of lactose ($5\ mg \cdot mL^{-1}$), 250 µL of ABTS solution ($1\ mg \cdot mL^{-1}$), 50 µL of glucose oxidase solution ($1\ mg \cdot mL^{-1}$) and 50 µL of HRP solution ($2\ mg \cdot mL^{-1}$) were placed in a quartz cuvette. All solutions were prepared in 50 mM sodium phosphate buffer at pH 7.5. Then, 100 µL of either buffer (for blank), commercial enzyme solution in buffer ($5\ mg \cdot mL^{-1}$) or $\mathbf{S1}_{\beta gal}$ suspension ($5\ mg \cdot mL^{-1}$) were added. The mixture was shaken and the absorbance at 418 nm was

monitored as a function of time. Whereas no change was observed in the absence of nanoparticles or commercial enzyme, a strong blue-green colour appeared in the presence of those. The increase in absorbance ($ABTS^{\cdot+}$ formation) as a function of time in the presence of **S1$_{\beta gal}$** and the commercial enzyme solution is depicted in **Figure S6**.

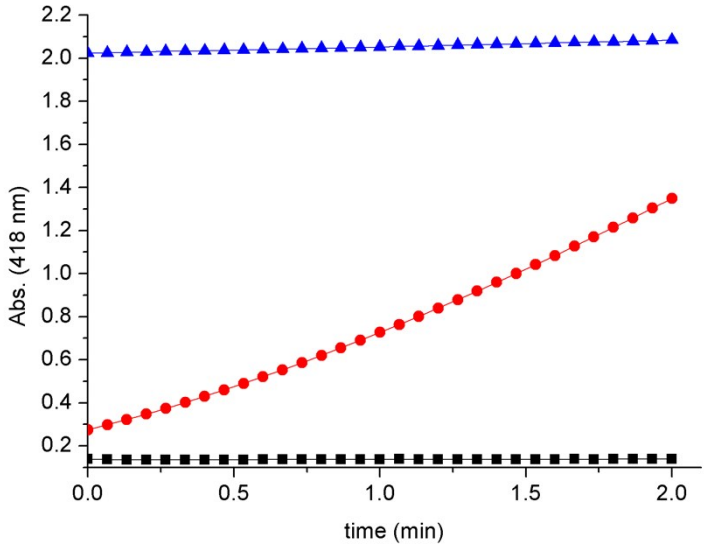

Figure S6. Monitoring of absorbance at 418 nm ($ABTS^{\cdot+}$ formation) due to β-galactosidase activity on nanoparticles **S1$_{\beta gal}$** (blue), commercial enzyme solution (red) and blank (black).

By applying the previously indicated formula (ε_{ABTS} at 418 nm = 36,000 $M^{-1} \cdot cm^{-1}$), the activity of β-galactosidase on **S1$_{\beta gal}$** was determined to be 0.001 U per mg of solid (0.006 $U \cdot mL^{-1}$ of solid suspension) whereas the activity of commercial β-galactosidase was determined to be 0.02 U per mg of commercial enzyme (0.11 $U \cdot mL^{-1}$ of enzyme solution). From this data, the corresponding amount of β-galactosidase on **S1$_{\beta gal}$** was estimated to be 56.10 mg of enzyme per g of solid.

The method used to test galactose oxidase activity is based on the oxidation of galactose by galactose oxidase leading to D-galacto-hexodialdose and hydrogen peroxide. Hydrogen peroxide reacts with ABTS (2,2'-azino-bis(3-ethylbenzothiazoline-6-sulfonic acid) diammonium salt) in the presence of peroxidase (HRP) to form a blue-green product ($ABTS^{\cdot+}$) that can be followed UV-visible spectrophotometry (λ_{abs} = 418 nm).

Reactions for assaying galactose oxidase activity:

$$D\text{-}galactose + O_2 + H_2O \xrightarrow{\text{Galactose oxidase}} D\text{-}galacturonic\ acid + D\text{-}galacto\text{-}hexadialdose + H_2O_2$$

$$H_2O_2 + ABTS \xrightarrow{\text{HRP}} ABTS^{\cdot+} + H_2O$$

In a typical experiment, 100 µL of galactose 20 mM (3.6 mg·mL^{-1}), 480 µL of ABTS solution (5 mg·mL^{-1}) and 10 µL of HRP solution (1 mg·mL^{-1}) were placed in a quartz cuvette. All solutions were prepared in 50 mM sodium phosphate buffer at pH 7.5. Then, 10 µL of either buffer (for blank), commercial enzyme (0.1 mg·mL^{-1}) or **S2$_{galox}$** (5 mg·mL^{-1}) were added. The mixture was shaken and absorbance at 418 nm was monitored as a function of time. Whereas no change was observed in the absence of nanoparticles or commercial enzyme, a strong blue-green colour appeared in the presence of those. The increase in absorbance ($ABTS^{\cdot+}$ formation) as a function of time in the presence of **S2$_{galox}$** and the commercial enzyme solution is depicted in **Figure S7**.

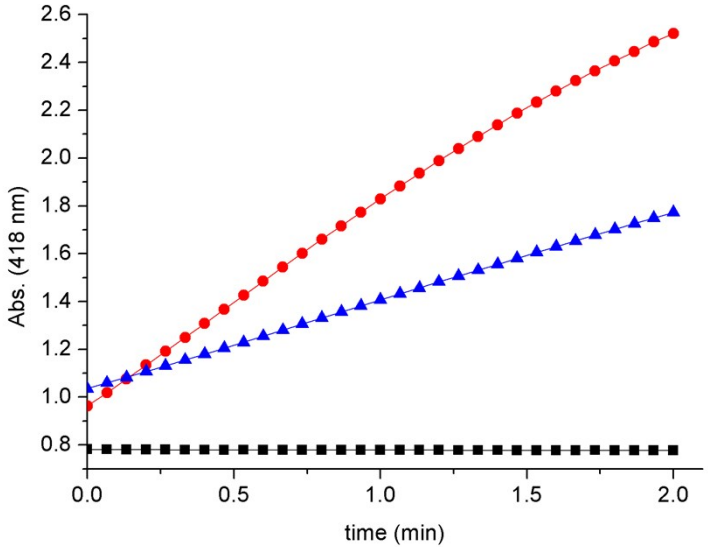

Figure S7. Monitoring of absorbance at 418 nm ($ABTS^{\cdot+}$ formation) due to galactose oxidase activity on nanoparticles **S2$_{galox}$** (blue), commercial enzyme (red) and blank (black).

By applying the previously indicated formula (ε_{ABTS} at 418 nm = 36,000 $M^{-1} \cdot cm^{-1}$), the activity of galactose oxidase on **S2$_{galox}$** was determined to be 0.124 U per mg of solid (0.620 U·mL^{-1} of solid suspension) whereas the activity of commercial galactose oxidase was determined to be 13.73 U per mg of commercial enzyme (1.33 U·mL^{-1} of enzyme solution). From this data, the corresponding amount of galactose oxidase on **S2$_{galox}$** was estimated to be 9.03 mg of enzyme per g of solid.

The method used to test esterase activity is based on the hydrolysis of 4-nitrophenyl butyrate by esterase into 4-nitrophenol (4-NP) and butyric acid. The yellow colour of 4-nitrophenol can be followed UV-visible spectrophotometry (λ_{abs} = 405 nm).

Reactions for assaying esterase activity:

$$4\text{-}nitrophenyl\ butyrate + H_2O \xrightarrow{\text{Esterase}} 4\text{-}nitrophenol + butyric\ acid$$

To check esterase activity, 100 µL of 4-nitrophenyl butyrate 10 mM (2.1 mg·mL^{-1} in 50 mM sodium phosphate buffer at pH 7.5) and 890 µL of 50 mM sodium phosphate buffer at pH 7.5 were placed in a quartz cuvette. Then, 10 µL of either, buffer (for blank), commercial enzyme solution (0.1 mg·mL^{-1}) or **S3$_{est}$** suspension (5 mg·mL^{-1}) were added. The mixture was shaken and absorbance at 405 nm was monitored as a function of time. Whereas no change was observed in the absence of nanoparticles or commercial enzyme, a strong yellow colour appeared in the presence of those. The increase in absorbance (4-nitrophenol formation) as a function of time in the presence of **S3$_{est}$** and the commercial enzyme solution is depicted in **Figure S8**.

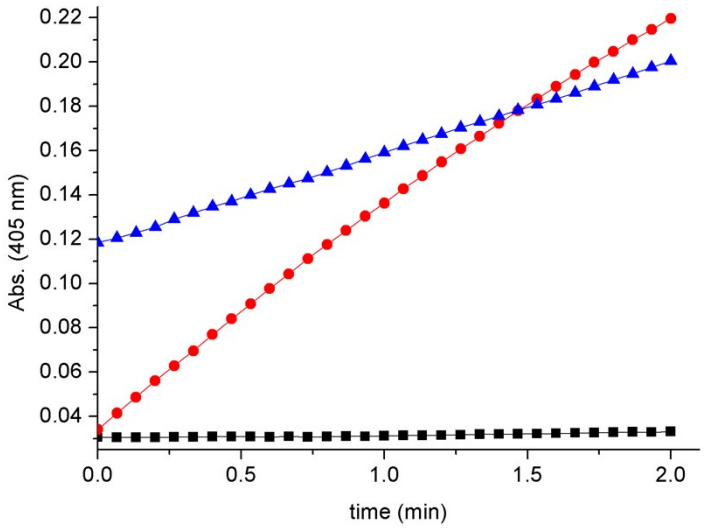

Figure S8. Monitoring of absorbance at 405 nm (4-nitrophenol formation) due to esterase activity on nanoparticles **S3$_{est}$** (blue), commercial enzyme (red) and blank (black).

By applying the previously indicated formula ($\varepsilon_{4\text{-NP}}$ at 405 nm = 5,000 M^{-1} · cm^{-1}), the activity of esterase on **S3$_{est}$** was determined to be 0.165 U per mg of solid (0.824 U·mL^{-1} of solid suspension) whereas the activity of commercial esterase was determined to be 18.62 U per mg of commercial enzyme (1.86 U·mL^{-1} of enzyme solution). From this data, the corresponding amount of esterase on **S3$_{est}$** was estimated to be 8.85 mg of enzyme per g of solid.

TEM-EDX mapping of the final nanodevices **S1$_{\beta gal}$**, **S2$_{galox}$** and **S3$_{est}$** confirmed the presence of the expected atoms in the solids. Images showed that gold surfaces were rich in sulfur atoms, strongly suggesting the preferential localization of the enzymes in the gold face (**Figure S9**, **S10** and **S11**) as they are immobilized by means of 3-mercaptopropionic acid. Moreover, the presence of sulfur atoms in the whole scaffold **S1 $_{\beta gal}$** is attributed to the disulfide bonds of the PEG moieties of the gatekeeper in the silica face while the slight signal of sulfur atoms in **S2$_{galox}$** and **S3$_{est}$** is attributed to the (3-mercaptopropyl)trimethoxysilane employed to attach the gold nanoparticles to the silica container

during the scaffold synthesis. Boron atoms and nitrogen atoms signals in **S2$_{galox}$** are due to the boronic esters and carbamate groups of the gatekeepers in **S2$_{galox}$**, whereas the abundance of nitrogen atoms in **S3$_{est}$** is attributed to the presence of benzimidazole moieties.

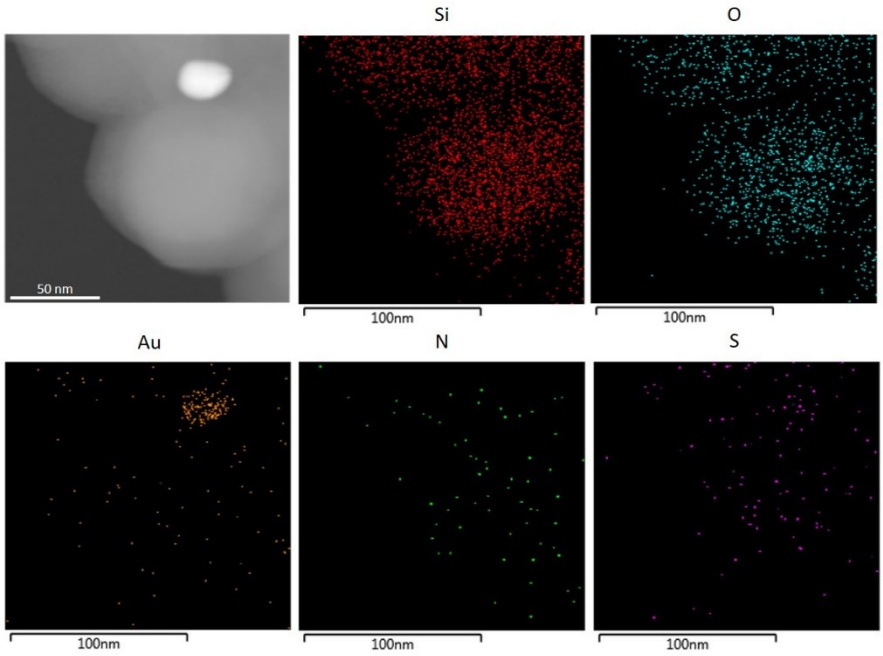

Figure S9. TEM-EDX element mapping of the nanodevice **S1$_{\beta gal}$**.

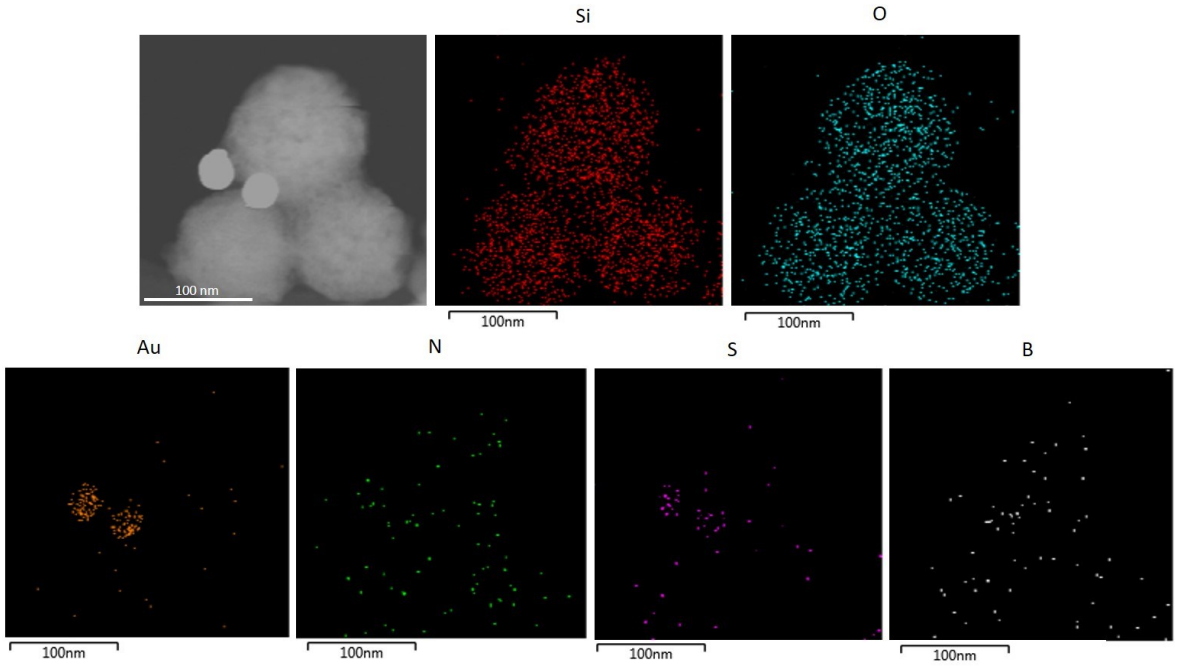

Figure S10. TEM-EDX element mapping of the nanodevice **S2$_{galox}$**.

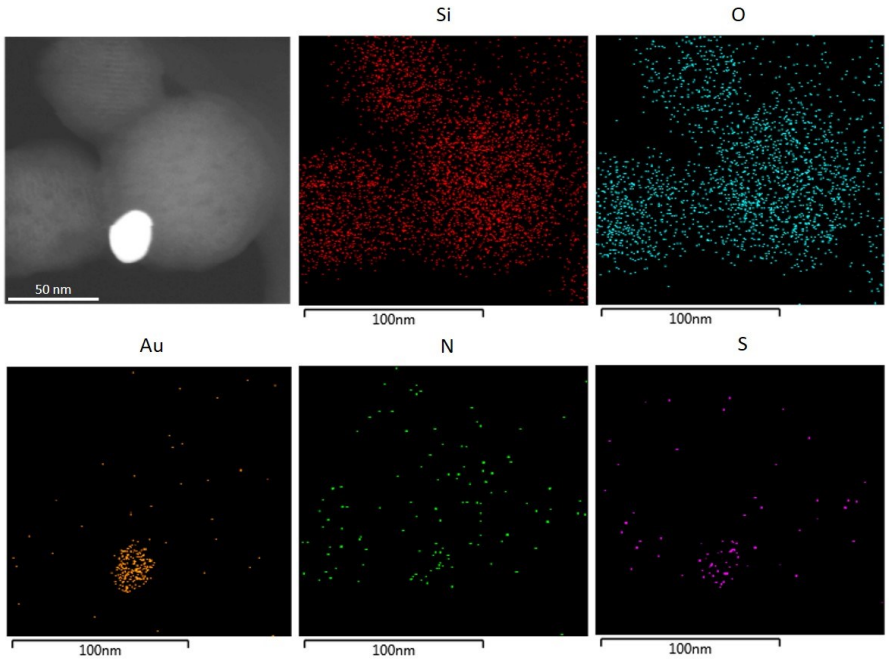

Figure S11. TEM-EDX element mapping of the nanodevice **S3$_{est}$**.

16. Release studies

Individual release studies

The corresponding refrigerated solution was washed first with an aqueous solution (pH 7.5, 20 mM Na_2SO_4), divided into two fractions and brought to certain final concentration. Both fractions were incubated shaking for 1 hour. Then, the input was added to one fraction (sample) while the same volume of aqueous solution was added to the other (blank). The addition of the input was considered as the beginning of the release experiment (time = 0 minutes). Samples were shaken over time and aliquots were taken at scheduled times, centrifuged (2 minutes, 12000 rpm) to remove the nanoparticles and the fluorescence was measured ($[Ru(bpy)_3]Cl_2$ λ_{exc} = 453 nm, λ_{em} = 595 nm). Final nanoparticle concentrations were 1 mg·mL^{-1} for **S1$_{\beta gal}$**; 2 mg·mL^{-1} for **S2$_{galox}$-dye** and 1 mg·mL^{-1} for **S3$_{est}$-dye**. Final input concentrations in each pair were TCEP 1 mM, galactose 50 mM and methyl 4-(bromomethyl)benzoate 1 mM + 2% of EtOH (to allow ester solubilization), respectively.

Additional individual studies

In order to confirm that each nanodevice delivery was only triggered by its corresponding stimulus, several positive (expected release) and negative controls (non-expected release) were carried out. For **S1$_{\beta gal}$**, galactose 50 mM, methyl 4-(bromomethyl)benzoate 1 mM + 2% of EtOH (negative controls) and tris(2-carboxyethyl)phosphine hydrochloride (TCEP) 1 mM (positive control) were tested as inputs. In

addition, it was also proved that high concentrations of lactose did not trigger cargo delivery by employing 5, 10 and 50 mM of lactose (negative controls). For **S2$_{galox}$-dye**, methyl 4-(bromomethyl)benzoate 1 mM + 2% of EtOH, TCEP 1 mM (negative control), galactose 50 mM and H_2O_2 50 mM (positive control) were tested as inputs. Galactose 50 mM was also tested with the nanodevice **S2-dye** lacking the enzyme. For **S3$_{est}$-dye**, TCEP 1 mM, galactose 50 mM (negative control), methyl 4-(bromomethyl)benzoate 1 mM + 2% of EtOH and HCl 1 mM (positive control) were tested as inputs. Methyl 4-(bromomethyl)benzoate 1 mM + 2% of EtOH was also tested with the nanodevice **S3-dye** lacking the enzyme.

In order to carry out these experiments, the corresponding refrigerated solution was washed with an aqueous solution (pH 7.5, 20 mM Na_2SO_4), divided into as many fractions as stimuli studied and brought to the final concentration (1 mg·mL^{-1} for **S1$_{\beta gal}$**, 2 mg·mL^{-1} for **S2$_{galox}$-dye** and 1 mg·mL^{-1} for **S3$_{est}$-dye**). All fractions were incubated shaking for 1 hour. Then, the inputs were added to the samples while the same volume of aqueous solution was added to the other fraction (blank). The addition of the inputs was considered as the beginning of the release experiment (time = 0 minutes). Samples were shaken over time and aliquots were taken at scheduled times, centrifuged (2 minutes, 12000 rpm) to remove the nanoparticles and the fluorescence was measured ($[Ru(bpy)_3]Cl_2$ λ_{exc} = 453 nm, λ_{em} = 595 nm). The results are shown in **Figures S12**, **S13** and **S14**.

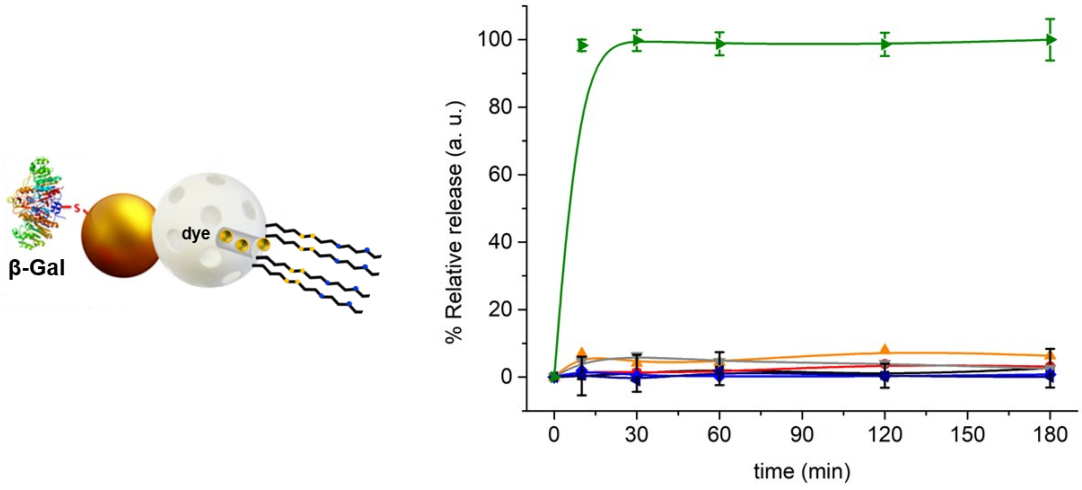

Figure S12. Normalized cargo release graphic from **S1$_{\beta gal}$** in the absence of input (black curve) and in the presence of galactose 50 mM (red), methyl 4-(bromomethyl)benzoate 1 mM + 2% of EtOH (orange); lactose 5 (grey), 10 (light blue) and 50 mM (dark blue) compared to the release in the presence of TCEP 1 mM (green). Error bars correspond to the s.d. from three independent experiments.

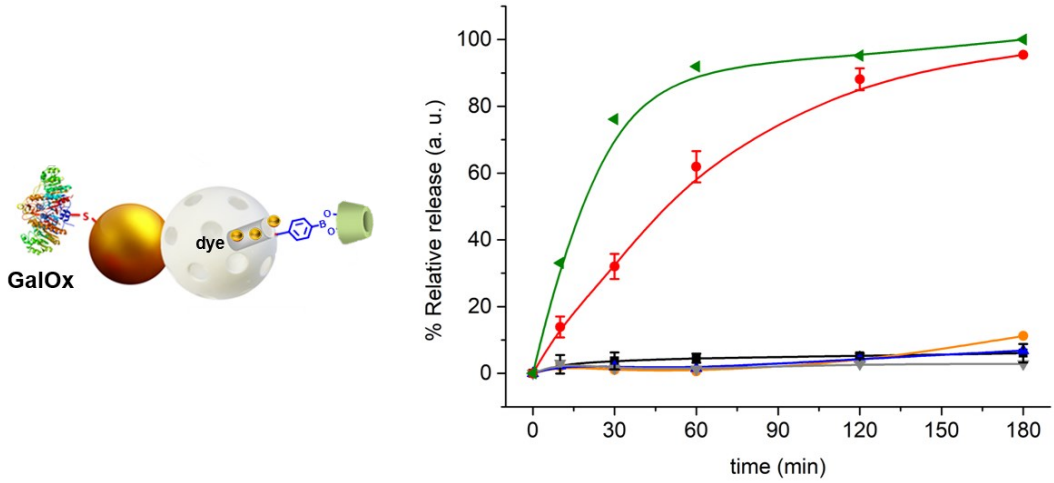

Figure S13. Normalized cargo release graphic from **S2$_{galox}$-dye** in the absence of input (black curve) and in the presence of methyl 4-(bromomethyl)benzoate 1 mM + 2% of EtOH (orange) , TCEP 1 mM (blue), galactose 50 mM (red) and H_2O_2 50 mM (green). Normalized cargo release from **S2-dye** (lacking the galox enzyme) in the presence of galactose 50 mM (grey) is also plotted. Error bars correspond to the s.d. from three independent experiments.

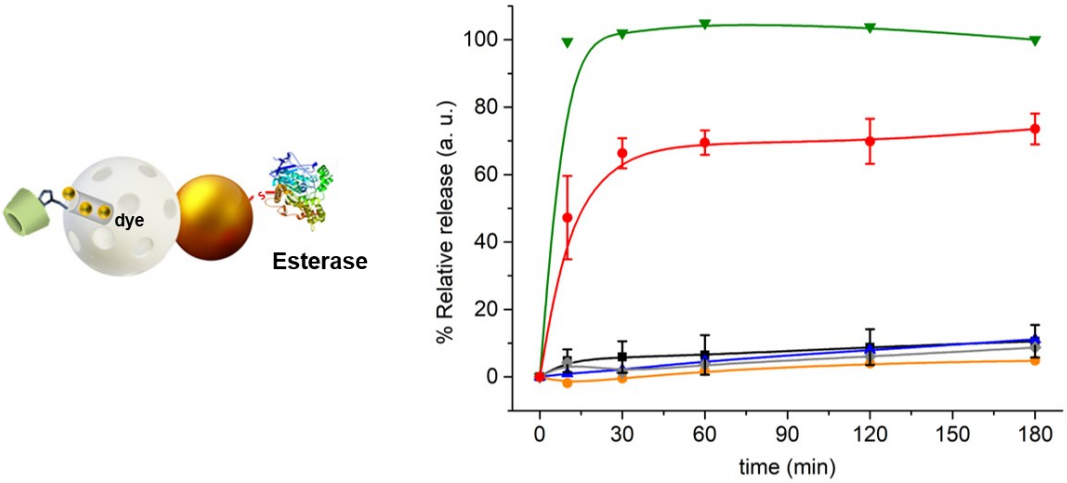

Figure S14. Normalized cargo release graphic from **S3$_{est}$-dye** in the absence of input (black curve) and in the presence of TCEP 1 mM (blue), galactose 50 mM (orange), methyl 4-(bromomethyl)benzoate 1 mM + 2% of EtOH (red) and HCl 1 mM (green). Normalized cargo release from **S3-dye** (enzyme missing) in the presence of methyl 4-(bromomethyl)benzoate 1 mM + 2% of EtOH (grey) is also plotted. Error bars correspond to the s.d. from three independent experiments.

Linear communication between pairs of nanoparticles

Each pair of the corresponding refrigerated solutions of nanoparticles were washed separately with an aqueous solution (pH 7.5, 20 mM Na_2SO_4) and incubated together shaking for 1 hour. Then, the mixture of both solids was divided into two fractions. Both fractions were incubated for another hour. Then, the input was added to one fraction (sample) while the same volume of aqueous solution was added to the other fraction (blank). The addition of the input was considered as the beginning of the release experiment (time = 0 minutes). Samples were shaken over time and aliquots were taken at scheduled

times, centrifuged (2 minutes, 12000 rpm) to remove the nanoparticles and the fluorescence was measured ($[Ru(bpy)_3]Cl_2$ λ_{exc} = 453 nm, λ_{em} = 595 nm). Final nanoparticle concentrations were 3/1 mg·mL^{-1} for **S1$_{\beta gal}$/S2$_{galox}$-dye** pair; 2.5/0.5 mg·mL^{-1} for **S2$_{galox}$/S3$_{est}$-dye** pair; and 1/1 mg·mL^{-1} for **S3$_{est}$/S1$_{\beta gal}$** pair. Final input concentrations were 50 mM of lactose, 50 mM of galactose and 2% of EtOH+1 mM of methyl 4-(bromomethyl)benzoate for each pair, respectively.

Circular communication experiments

S1$_{\beta gal}$, **S2$_{galox}$** and **S3$_{est}$** were washed separately with an aqueous solution (pH 7.5, 20 mM Na_2SO_4) and separately incubated shaking for 1 hour. Then, the three solutions were mixed and equally divided into two fractions, each of them with a concentration of 3 mg·mL^{-1} of **S1$_{\beta gal}$**, 2.25 mg·mL^{-1} of **S2$_{galox}$** and 0.75 mg·mL^{-1} of **S3$_{est}$**. Both fractions were incubated for another hour with 2% of EtOH. Then, the input (lactose, final concentration 50 mM) was added to one fraction (sample) while the same volume of aqueous solution was added to the other fraction (blank). The addition of the input was considered as the beginning of the release experiment (time = 0 minutes). Samples were shaken over time and aliquots were taken at scheduled times, centrifuged (2 minutes, 12000 rpm) to remove the nanoparticles and the fluorescence was measured ($[Ru(bpy)_3]Cl_2$ λ_{exc} = 453 nm, λ_{em} = 595 nm).

Control experiments

The same procedure as described above for the "*Circular communication experiments*" was followed with suspensions of:

S1/S2$_{galox}$/S3$_{est}$
S1$_{\beta Gal}$/S2/S3$_{est}$
S1$_{\beta Gal}$/S2$_{galox}$/S3
S1$_{\beta Gal}$/S2$_{blank}$/S3$_{est}$
S1$_{\beta Gal}$/S2$_{galox}$/S3$_{blank}$
S1/S2/S3/free enzymes
S1/S2$_{galox}$/S3$_{est}$/free β-galactosidase
S1$_{\beta Gal}$/S2/S3$_{est}$/free galactose oxidase
S1$_{\beta Gal}$/S2$_{galox}$ /S3/free esterase

For the release experiments in the community **S1/S2/S3**/free enzymes, **S1/S2$_{galox}$/S3$_{est}$**/free β-galactosidase, **S1$_{\beta Gal}$/S2/S3$_{est}$**/free galactose oxidase and **S1$_{\beta Gal}$/S2$_{galox}$ /S3**/free esterase, **S1**, **S2** and **S3** (3 mg·mL^{-1}, 2.25 mg·mL^{-1} and 0.75 mg·mL^{-1}, respectively) were placed in a recipient with β-galactosidase (0.006 U·mL^{-1}), galactose oxidase (0.62 U·mL^{-1}) and/or esterase (0.82 U·mL^{-1}). The results are plotted in **Figure 6** (main text).

Efficiency experiments

The same experimental procedure as described above for the "*Circular communication experiments*" was followed. The same concentrations of nanoparticles and inputs (3 mg·mL^{-1} of **S1$_{\beta gal}$**, 2.25 mg·mL^{-1} of **S2$_{galox}$**, 0.75 mg·mL^{-1} of **S3$_{est}$** and 50 mM of input) were also employed in suspensions of:

1) **S1$_{\beta Gal}$** with no input + 2% of EtOH - [blank]
2) **S1$_{\beta Gal}$** + TCEP 50 mM + 2% of EtOH - [set as 100% efficiency]
3) **S3$_{est}$/S1$_{\beta Gal}$** + methyl 4-(bromomethyl)benzoate 50 mM + 2% of EtOH - [sequence **3-1**]
4) **S2$_{galox}$/S3$_{est}$/S1$_{\beta Gal}$** + galactose 50 mM + 2% of EtOH - [sequence **2-3-1**]
5) **S1$_{\beta Gal}$/S2$_{galox}$/S3$_{est}$** + lactose 50 mM + 2% of EtOH - [sequence **1-2-3-1**]

The communication efficiency of each sequence (**Figure 7A** in main text) was calculated by relativizing the output (amount of cargo delivered) of the sequence to the maximum possible output (cargo released from suspension 2 set as 100% efficiency) and considering the blank as background level:

$$Relativization\ (\%): \frac{Output\ signal\ (a.u.) - blank\ signal\ (a.u.)}{(100\%\ efficiency\ signal\ (a.u.) - blank\ signal\ (a.u.)} x\ 100$$

Based on these experiments, we calculated the efficiency of each connection process (Process efficiency) in the circular communication system (**Figure 7B** in main text) by applying the following set of equations:

*% Communication efficiency **1-2-3-1** = % Efficiency [**1-2** process] x % Efficiency [**2-3** process] x % Efficiency [**3-1** process] x 10^{-4}*

*% Communication efficiency **2-3-1** = % Efficiency [**2-3** process] x % Efficiency [**3-1** process] x 10^{-2}*

*% Communication efficiency **3-1** = % Efficiency [**3**-**1** process]*

In order to determinate the chemical information loss, we represented in **Figure S15** the difference between the maximum ideal communication efficiency (100%) and the obtained efficiency value for each sequence [**1-2-3-1** (**S1$_{\beta gal}$-S2$_{galox}$-S3$_{est}$-S1$_{\beta gal}$**), **2-3-1** (**S2$_{galox}$-S3$_{est}$-S1$_{\beta gal}$**) and **3-1** (**S3$_{est}$-S1$_{\beta gal}$**)] at 24h (see **Figure 7A** in the manuscript).

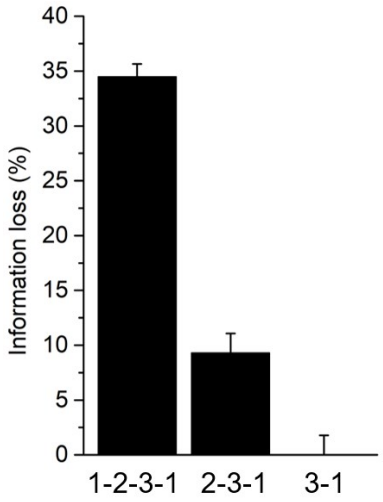

Figure S15. Representation of the chemical information loss in each sequence of the communication system after 24h. Error bars correspond to the s.d. from two independent experiments.

Boolean logic table

Table S4. Summary of the behaviour of the circular communication network in Boolean logic terms. The presence or absence of the input (lactose), encapsulated cargo or enzymes immobilized on the nanoparticles is represented by "1" (presence) and "0" (absence), respectively. The output signal is considered 0 when the normalized quantification of the $[Ru(bpy)_3]Cl_2$ fluorescence intensity is less than 30% of that found for the complete network.

Entry	(External trigger) Lactose	β-galactosidase	Galactose oxidase	(Cargo 2) Benzoate derivative	Esterase	(Cargo 3) TCEP	(Output) $[Ru(bpy)_3]Cl_2$ release
1	0	0	0	0	0	0	0
2	0	0	0	0	0	1	0
3	0	0	0	0	1	0	0
4	0	0	0	0	1	1	0
5	0	0	0	1	0	0	0
6	0	0	0	1	0	1	0
7	0	0	0	1	1	0	0
8	0	0	0	1	1	1	0
9	0	0	1	0	0	0	0
10	0	0	1	0	0	1	0
11	0	0	1	0	1	0	0
12	0	0	1	0	1	1	0
13	0	0	1	1	0	0	0
14	0	0	1	1	0	1	0
15	0	0	1	1	1	0	0
16	0	0	1	1	1	1	0
17	0	1	0	0	0	0	0
18	0	1	0	0	0	1	0
19	0	1	0	0	1	0	0
20	0	1	0	0	1	1	0
21	0	1	0	1	0	0	0
22	0	1	0	1	0	1	0
23	0	1	0	1	1	0	0
24	0	1	0	1	1	1	0
25	0	1	1	0	0	0	0
26	0	1	1	0	0	1	0

Entry	(External trigger) Lactose	β-galactosidase	Galactose oxidase	(Cargo 2) Benzoate derivative	Esterase	(Cargo 3) TCEP	(Output) $[Ru(bpy)_3]Cl_2$ release
27	0	1	1	0	1	0	0
28	0	1	1	0	1	1	0
29	0	1	1	1	0	0	0
30	0	1	1	1	0	1	0
31	0	1	1	1	1	0	0
32	0	1	1	1	1	1	0
33	1	0	0	0	0	0	0
34	1	0	0	0	0	1	0
35	1	0	0	0	1	0	0
36	1	0	0	0	1	1	0
37	1	0	0	1	0	0	0
38	1	0	0	1	0	1	0
39	1	0	0	1	1	0	0
40	1	0	0	1	1	1	0
41	1	0	1	0	0	0	0
42	1	0	1	0	0	1	0
43	1	0	1	0	1	0	0
44	1	0	1	0	1	1	0
45	1	0	1	1	0	0	0
46	1	0	1	1	0	1	0
47	1	0	1	1	1	0	0
48	1	0	1	1	1	1	0
49	1	1	0	0	0	0	0
50	1	1	0	0	0	1	0
51	1	1	0	0	1	0	0
52	1	1	0	0	1	1	0
53	1	1	0	1	0	0	0
54	1	1	0	1	0	1	0
55	1	1	0	1	1	0	0
56	1	1	0	1	1	1	0
57	1	1	1	0	0	0	0
58	1	1	1	0	0	1	0
59	1	1	1	0	1	0	0
60	1	1	1	0	1	1	0
61	1	1	1	1	0	0	0
62	1	1	1	1	0	1	0
63	1	1	1	1	1	0	0
64	1	1	1	1	1	1	1

Table S5. Relative dye release when a component of the system is missing.

	Missing element	**Relative output (%)**
-	100 ± 2.0	
Lactose (External trigger)	19.6 ± 5.2	
β-galactosidase	16.2 ± 3.1	
Galactose oxidase	16.4 ± 3.0	
Benzoate derivative (Cargo 2)	25.6 ± 12.0	
Esterase	29.3 ± 1.0	
TCEP (Cargo 3)	25.6 ± 7.2	

17. Supplementary References

1 T. M. Godoy-Reyes, A. Llopis-Lorente, A. García-Fernández, P. Gaviña, A. M. Costero, R. Villalonga, F. Sancenón and R. Martínez-Máñez, *Org. Chem. Front.*, 2019, **6**, 1058.

2 J. A. Turkevich, P. C. Stevenson and J. Hillier, *Discuss. Faraday Soc.*, 1951, **11**, 55.

3 G. Frens, *Nat. Phys. Sci.*, 1973, **241**, 20.

4 R. Villalonga, P. Díez, A. Sánchez, E. Aznar, R. Martínez-Máñez and J. M. Pingarrón, *Chem. Eur. J.,* 2013, **19**, 7889.

5 K. L. Kelly, E. Coronado, L. L. Zhao and G. C. Schatz, *J. Phys. Chem. B*, 2003, **107**, 668.